Role of plant growth promoting bacteria in driving speciation gradients across soil-rhizosphere-plant interfaces in zinc-contaminated soils

Role of plant growth promoting bacteria in driving speciation gradients across soil-rhizosphere-plant interfaces in zinc-contaminated soils

Nyekachi C. Adele[a], Bryne T. Ngwenya[a*], Kate V. Heal[a] and J. Frederick W. Mosselmans[b]

[a]School of GeoSciences, University of Edinburgh, Edinburgh, UK

[b]Diamond Light Source, Harwell Science and Innovation Campus, Didcot, UK

[*]Corresponding author

Abstract

Inoculation of soil or seeds with plant growth promoting bacteria ameliorates metal toxicity to plants by changing metal speciation in plant tissues but the exact location of these changes remains unknown. Knowing where the changes occur is a critical first step to establish whether metal speciation changes are driven by microbial metabolism or by plant responses. Since bacteria concentrate in the rhizosphere, we hypothesised steep changes in metal speciation across the rhizosphere. We tested this by comparing speciation of zinc (Zn) in roots of *Brassica juncea* plants grown in soil contaminated with 600 mg kg^{-1} of Zn with that of bulk and rhizospheric soil using synchrotron X-ray absorption spectroscopy (XAS). Seeds were either uninoculated or inoculated with *Rhizobium leguminosarum* bv. *trifolii* and Zn was supplied in the form of sulfide (ZnS nanoparticles) and sulfate ($ZnSO_4$). Consistent with previous studies, Zn toxicity, as assessed by plant growth parameters, was alleviated in *B. juncea* inoculated with *Rhizobium leguminosarum*. XAS results showed that in both ZnS and $ZnSO_4$ treatments, the most significant changes in speciation occurred between the rhizosphere and the root, and involved an increase in the proportion of organic acids and thiol

complexes. In ZnS treatments, Zn phytate and Zn citrate were the dominant organic acid complexes, whilst Zn histidine also appeared in roots exposed to $ZnSO_4$. Inoculation with bacteria was associated with the appearance of Zn cysteine and Zn formate in roots, suggesting that these two forms are driven by bacterial metabolism. In contrast, Zn complexation with phytate, citrate and histidine is attributed to plant responses, perhaps in the form of exudates, some with long range influence into the bulk soil, leading to shallower speciation gradients.

Keywords: *Brassica juncea*, nanoparticles, phytoremediation, X-ray absorption spectroscopy, zinc

1. Introduction

The rhizosphere is a narrow region of soil surrounding the plant-root environment and is characterised by microbial populations that exceed the populations in nearby bulk soil (Helliwell et al., 2017) due to production of exudates by plants, which microbes use as metabolites (Lee et al., 2019). As a result, the rhizosphere is an active zone of plant-microbe interactions which facilitates a large number of processes that may be beneficial, harmful or neutral to both the plant and the microbe (Bishnoi, 2015; Buée et al., 2009). Amongst the plant-beneficial attributes of such interactions are nutrient acquisition, plant growth promotion, pest control, stress alleviation (Adediran et al., 2016a; Adele et al., 2018; Glick, 2014) and degradation of toxic substances (Jambon et al., 2018). An understanding of plant-microbe interactions in the rhizosphere is therefore essential for improving plant health, ecosystem functioning and environmental health (Helliwell et al., 2017; Wu et al., 2017).

Toxic metals, which are being continuously added to soils through industrial and transport emissions, increased production and use of nanomaterials, mining activities, waste and sewage disposal, fertilisers and pesticides, and atmospheric deposition (Auffan et al., 2009; Hernandez-Viezcas et al., 2011; Lv et al., 2019; Pradas del Real et al., 2016), pose a particularly persistent environmental problem because they are not degradable and thus accumulate in the environment (Rizwan et al., 2017). Metal toxicity and bioavailability can be alleviated by changing its chemical speciation (Adele et al., 2018). Differences in chemical and physical characteristics across the rhizosphere (Chiang et al., 2006; Rico et al., 2018) are manifest in the development of steep gradients in metal concentration, pH, redox potential, pO_2, pCO_2 and organic ligand concentrations between the plant root and soil (Guo et al., 2019; Jilling et al., 2018; Ma et al., 2018; Zhalnina et al., 2018; Zhao et al., 2016), and are likely to lead to changes in metal speciation. For example, the grass species *Festuca rubra* (red fescue) and *Agrostis tenuis* (colonial bent grass) accelerated the weathering of ZnS when grown on contaminated dredged sediment, thus increasing Zn bioavailability in the rhizosphere (Panfili et al., 2005). However, after 2 years of plant growth, μm-sized Mn-Zn black precipitates were observed on the surface of *Festuca rubra* roots, which were identified as a Zn-rich phyllomanganate, suggesting that Zn biomineralisation by plants is a defence mechanism against metal toxicity (Lanson et al., 2008). In another study, changes in metal solubility in rhizobox experiments were attributed to altered soil solution pH and dissolved organic carbon arising from *B. juncea* root exudates (Kim et al., 2010).

The presence of microbes is likely to amplify these gradients because of increased metabolic activities that change the balance between reductants and terminal electron acceptors, the latter of which include redox-sensitive trace metals (Gadd, 2010). Many studies have demonstrated that the presence of microbes within the soil-root environment (rhizospheric or

endophytic) can influence both the bioavailability and toxicity of metals within plant tissues, ultimately increasing metal bioaccumulation and improving plant health (Adediran et al., 2016a; Adele et al., 2018; Luo et al., 2011; Sessitsch, et al., 2013). The traditional explanation for these microbial-induced effects is biochemical changes in the soil-root environment arising from microbial activity, resulting in prevention of excessive secretion of ethylene by plants, optimum production of plant essential hormones (e.g. cytokinins and gibberellins), and improved release and utilisation of essential nutrients (Bardgett and van der Putten, 2014; Khanna et al., 2019). However, recent advances in molecular level studies, especially those using synchrotron-based spectroscopies, increasingly invoke changes in speciation of the metal as the principal driver of metal bioavailability and toxicity alleviation (Adediran et al., 2016a; Kopittke et al., 2011).

Our group has been studying the role of rhizospheric and endophytic bacteria on Zn uptake by *B. juncea* (Adediran et al., 2015, 2016a,b; Adele et al., 2018). Whilst Zn is an essential micronutrient required for healthy plant growth, excess Zn can be detrimental, inducing impaired plant growth, and reduced chlorophyll and seed production, resulting in chlorosis and plant death (Broadley et al., 2007; Rascio and Navari-Izzo, 2011). Inoculation of *B. juncea* seeds with bacteria improved plant growth in Zn-contaminated soil but, paradoxically, improved growth was associated with increased Zn bioaccumulation in plant tissue (Adele et al., 2018). We hypothesised that toxicity amelioration was driven by bacteria-induced changes in Zn speciation, and subsequent synchrotron-based micro X-ray fluorescence (μ-XRF) and micro X-ray absorption near edge structure (μ-XANES) analysis of roots showed that bacterial inoculation significantly increased the proportion of Zn complexed with cysteine-rich ligands (Adediran et al., 2015, 2016a; Adele et al., 2018). These changes were replicated regardless of whether Zn was applied in dissolved or nanoparticulate form (Adele

et al., 2018), although the proportions depended on the bacterial species used (Adediran et al., 2015).

Major questions remain about the exact mechanisms by which bacteria effect such changes in metal speciation. One question is whether the bacteria themselves synthesise the ligands that complex Zn, perhaps as a form of metabolic response to toxic metal exposure (Adediran et al., 2016a; Chandrangsu et al., 2017). Answering this question requires the isolation of bacterial metabolic responses from those of the plants, which also deploy cysteine-rich ligands, including glutathione and phytochelatins for metal detoxification (Bhattacharjee and Rosen, 2007; Feldman et al., 2018; Khan et al., 2018; Mesa et al., 2017). The other question is determining the locus of the speciation changes, and whether the changes are driven by plant responses or microbial processes. If bacteria synthesise their own ligands, we would expect transformations to occur throughout the bulk soil. Alternatively, transformation occurs exclusively at the soil-root interface where microbes congregate, changing metal speciation. Adediran et al. (2016a) showed that bacteria co-localised with Zn in the rhizosphere of *B. juncea*, suggesting that metal speciation changes occur in the rhizosphere before plant uptake, a hypothesis which was tested in this study by comparing Zn speciation amongst bulk soil, rhizosphere and plant roots using X-ray absorption spectroscopy (XAS). Specific objectives were to: (i) investigate whether there are root-induced speciation changes of different Zn forms in the rhizosphere; (ii) determine whether such changes affect the uptake, accumulation and distribution of Zn in the plant; and (iii) investigate the role of *Rhizobium leguminosarum* bv. *trifolii* in modifying speciation across the soil-rhizosphere-plant interface.

Some previous studies have used selective extractions to characterise speciation gradients around the rhizosphere, but these only yield bulk phase associations rather than specific

chemical species, which XAS analysis can provide (Panfili et al., 2005). Indeed, XAS analysis has been used to significantly advance understanding of metal associations as well as chemical speciation in plant tissues (Salt et al., 1999), in the rhizosphere around plant roots (Medas et al., 2015; Terzano et al., 2008), and in the soils in which plants grow, including metal-mine waste areas (Boi et al., 2020; Medas et al., 2015). Very few studies have included the effects of plant-growth promoting bacteria, notably Medas et al. (2015), where the chemical speciation and mineralogical association of Zn in the rhizosphere and roots was controlled by plant-driven biomineralisation and/or plant exudates with no demonstrable involvement of bacteria. By using XAS analysis of samples spanning the bulk soil through the rhizosphere to the root tissue, we are able to assess not only the importance of the rhizosphere in changing Zn speciation but also to differentiate between plant and bacteria dominated speciation.

2. Materials and Methods

2.1 Experimental materials

This study focused on contamination by soluble Zn (in the form of $ZnSO_4.7H_2O$, Sigma Aldrich, UK) and ZnS nanoparticles. Zinc sulfide NPs (ZnS NPs) are rapidly increasing in the environment due to their multi-faceted applications such as in the pharmaceutical and cosmetic industries, biosensors, nanogenerators, and field emitters amongst others (Biruntha et al., 2020; Fang et al., 2011). ZnS was also used as a nanoparticle model relating to mine waste contamination. ZnS in the form of sphalerite is the most common form in which Zn is mined and therefore prevalent in mining impacted soils and has received increasing attention, although it may not necessarily occur in nanoparticulate form. For this study, ZnS nanoparticles were synthesised in the laboratory using a chemical precipitation method (Adele et al., 2018; Ganguly et al., 2014). Mean nanoparticle diameter was 8.65 nm, although

some aggregation was observed (see Supplementary Material S1 for details). Topsoil (Westland Horticulture Ltd., UK) was amended with 10% sand to improve drainage, and then air dried, crushed, and passed through a 2 mm stainless steel sieve. Measured soil physicochemical properties before amendment are reported in Supplementary Material Table S1. The air-dried soil was amended with 600 mg Zn kg^{-1} in the form of $ZnSO_4$, or ZnS nanoparticles. The Zn concentration chosen was sufficient to trigger toxic effects in plants without completely curtailing growth and also for XAS analysis of plant and soil samples (Adele et al., 2018). *Brassica juncea* (L.) Czern (hereafter *B. juncea*) was chosen for this study as a suitable candidate plant for remediation of Zn-contaminated soil or sediment (Qu et al., 2012; Wang et al., 2009). Seeds of *B. juncea* were purchased (Sow Seeds Ltd., UK) and stored in a clean plastic bag in the dark at room temperature (14-16 °C) until required. *Rhizobium leguminosarum* bv. *trifolii* (hereafter *R. leguminosarum*) was selected for bacterial inoculation due to its tolerance to Zn and demonstrated ability to promote growth of *B. juncea* (Adediran et al., 2016a; Adele et al., 2018).

2.2 Plant growth experiment design and set-up

The plant growth experiment (detailed in Supplementary Material S2) contained six treatments (including controls), each containing three replicates, in which *B. juncea* were grown in pots exposed to the different Zn species with and without the presence of bacteria. Briefly, sterilised air-dried soil was contaminated with 600 mg Zn kg^{-1} of $ZnSO_4$, or ZnS nanoparticles. pH was determined in two subsamples of the soil from each treatment after amendment in a 1:2 (fresh soil mass:deionised water volume) suspension. The mixture was stirred and shaken for 30 min before pH measurement using an electrode calibrated using pH 7.0 and 4.0 buffer solutions. Bacterial inoculation of *B. juncea* seeds involved surface sterilisation with 5% NaClO for 15 min, then washing three times with sterile deionised

175 water, before soaking for 4 h in 10 mL *R. leguminosarum* bacterial suspension. Uninoculated
176 seeds were soaked in sterilised deionised water for the same duration. One kg of spiked or
177 unspiked soil (control) was placed in 2.15 L pots and left to equilibrate for 1 week before
178 sowing five seeds in each pot. Seedlings were thinned out to three plants per pot at 12 days
179 after planting. Pots were distributed randomly in the greenhouse space and irrigated
180 individually with tap water twice a week. Greenhouse conditions were mean 21 °C daytime
181 and 18 °C night time temperatures, with a photoperiod of 18 h day^{-1} at a photosynthetic
182 photon flux density of 150 µmol m^{-2} s^{-1} provided by cool white fluorescent bulbs. Metal-
183 related phytotoxicity was evaluated by measuring plant height weekly, and root length and
184 dry biomass at the end of the experiment (6 weeks after seed planting), and through visual
185 observations such as leaf chlorosis and necrosis.
186
187 **2.3 Plant harvest, rhizospheric and bulk soil sampling and analysis**
188 All plants were harvested 6 weeks after planting. Shoots were separated from roots with
189 scissors. Rhizospheric soil was obtained as a composite sample of the loosely adhering soil
190 material obtained by shaking by hand the roots of the three plants in each pot. Bulk soil was
191 collected from outside the rhizosphere. Roots were washed gently with tap water and
192 stretched out for root length measurement. All samples were transferred to paper bags and
193 oven dried at 70 °C to constant weight, before grinding using mortar and pestle. Total Zn
194 concentrations in duplicate subsamples of the ground plant materials, bulk and rhizospheric
195 soil (mixed from the three replicate pots for each treatment) were determined as described by
196 Allen et al. (1974). Six mL concentrated HCl and 2 mL HNO_3 were used for digestion of 0.5
197 g ashed soil samples and 2 mL concentrated H_2SO_4 and 0.75 mL H_2O_2 (30%) for digestion of
198 0.1 g plant material samples. Zn concentrations in the digests were determined (following
199 filtration with 0.45 µm syringe filters) by inductively coupled plasma-optical emission

spectrometry (ICP-OES, PerkinElmer Optima 5300DV) using the Zn 206.200 nm line. Calibration standards (0.001-2 mg Zn L^{-1}) were prepared from Zn stock standard solution and calibration curves required an r^2 value ≥ 0.9999. Quality control checks comprised analysis of blanks and an external standard (Merck ICP Multi element standard solution VI CertiPUR®). Zinc concentrations measured in digest blanks were subtracted from the sample results. Zinc contents were expressed as mg kg^{-1} (dry weight) as the mean of the two subsamples for each treatment. Fresh bulk and rhizosphere soil were homogenised separately for pH determination in two subsamples in suspension as already described in section 2.2.

2.4 X-ray absorption spectroscopy (XAS) of bulk and rhizospheric soil and plant roots

XAS was used to investigate the distribution and speciation of Zn in bulk soil, rhizospheric soil and plant root samples on Beamline B18 at the Diamond Light Source, Didcot, UK. Samples and Zn reference standards were prepared and analysed as detailed in Supplementary Material S3. Duplicate samples were analysed of roots and rhizospheric soil in the uninoculated and inoculated ZnS treatments and the inoculated $ZnSO_4$ treatments, where the greatest changes in Zn speciation were expected. To assess Zn speciation, all X-ray absorption near edge structure (XANES) spectra collected from the samples and standards were normalised and aligned. Linear Combination Fitting (LCF, Athena IFFEFIT software; Ravel and Newville, 2005) was used to quantify the relative proportions of Zn reference compounds within the samples. The goodness of fit was determined from the residual *R*-factor between the sample spectrum and the spectrum fitted to a combination of Zn standards (Eq. 1), where a lower *R*-factor represents the best fit between the sample spectrum and the fitted spectrum:

$$R = \frac{\sum(\text{data} - \text{fit})^2}{\sum(\text{data})^2} \quad \text{Eq. 1}$$

225 **2.5 Data analysis**

226 The means and standard error (SE) of plant height, root length, dry shoot and root biomasses,
227 and metal concentrations in plant materials and bulk and rhizospheric soil were calculated for
228 each treatment. Statistical analyses were conducted using Minitab v.18 (Minitab TM Inc.,
229 State College, PA), with significance level $p < 0.05$. Datasets were tested for normality with
230 the Anderson-Darling test and those that were not normally distributed were transformed for
231 statistical analysis. General linear models (GLM) followed by Tukey multiple comparison
232 tests were used to identify any significant differences between treatments and controls on
233 these. All models contained factors of Zn exposure, bacterial inoculation, and their
234 interaction, and additionally soil type (bulk vs. rhizospheric) for the soil Zn concentration
235 model.

236

237 **3. Results and Discussion**

238 **3.1 Plant growth and health**

239 The effects of Zn and inoculation with *R. leguminosarum* on the growth and health of *B.*
240 *juncea* was monitored weekly for 6 weeks after planting. Plant height was similar in all
241 treatments until week 3, when the growth of plants exposed to Zn started to lag behind the
242 control plants, particularly the uninoculated $ZnSO_4$-treated plants which displayed mild
243 yellowing of leaves from week 4. Plant growth results at the end of the experiment in week 6
244 are shown in Fig. 1. Inoculation with *R. leguminosarum* and Zn exposure each had significant
245 effects on plant height (GLM: r^2 (adjusted) = 50.6%, $p = 0.048$ and 0.005, respectively), with
246 significantly greater plant height in the bacterial inoculation than in the uninoculated
247 treatments. The control plants were significantly taller than those exposed to Zn, but there
248 was no significant difference in plant height between the $ZnSO_4$ and ZnS treatments (Fig. 1a).
249 *B. juncea* root length was the plant growth parameter most adversely affected by Zn exposure

after 6 weeks growth (Fig. 1b, Fig. S1). The GLM (r^2 (adjusted) = 80.2%) showed that bacterial inoculation and Zn exposure each had significant effects on root length (p = 0.001 and <0.001, respectively). Roots in the *R. leguminosarum* treatments were significantly longer than in the uninoculated treatments. In the uninoculated plants exposed to Zn, roots were significantly shorter compared to the control plants, but root lengths in the inoculated plants exposed to Zn did not differ from those of the uninoculated control plants. *B. juncea* shoot dry biomass at the end of the experiment was an order of magnitude greater than root dry biomass (Fig. 1c-d). Separate GLMs for shoot and root biomasses (r^2 (adjusted) = 39.3% and 49.5%, respectively) showed that they were both significantly affected by Zn exposure (p = 0.021 and 0.004, respectively) but not by bacterial inoculation. Tukey multiple comparisons between Zn treatments (not shown) showed significantly lower shoot biomass in the $ZnSO_4$ plants compared to the control and ZnS treatments which were not significantly different, whereas root biomasses in both the Zn-exposed treatments did not differ and were significantly lower than in the control plants.

Figure 1 here

Overall, across all individual treatments, plant height, root length, shoot and root biomass were significantly lower in the uninoculated $ZnSO_4$ treatment compared to the inoculated control, whilst the only significant difference in plant growth parameters in the ZnS treatments compared to the control plants was shorter root length in the uninoculated ZnS treatment (Fig. 1b). This is consistent with $ZnSO_4$ being more toxic to plants than ZnS nanoparticles-amended soil, attributable to the higher solubility of $ZnSO_4$, with dissolved Zn impairing plant metabolism and interfering with the absorption of essential elements (Rout and Das, 2009). Dissolution of ZnS nanoparticles is generally dependent on particle size

(Zhang et al., 2010). Thus, differences in solubility between ZnS and $ZnSO_4$ would have been amplified by the aggregated state of the nanoparticles in our study (Fig S1), effectively increasing their hydrodynamic particle size and reducing their surface energy (Eskelsen et al., 2018). Bacterial inoculation compensated for the negative effect of Zn on *B. juncea* growth, increasing plant height in the inoculated $ZnSO_4$ treatment and root length in both Zn treatments so that they were not significantly different from those of uninoculated control plants (Fig. 1a-b). Whilst the GLMs showed that bacterial inoculation and Zn exposure individually had a significant effect on nearly all plant growth parameters in the experiment, their interaction terms in all GLMs were non-significant (p >0.05), indicating no significant interaction effect of bacterial inoculation and Zn exposure on *B. juncea* growth. The plant growth experiment results are consistent with our previous studies (Adediran et al., 2015; Adele et al., 2018). In those studies, bacteria were demonstrated to induce changes in the speciation of Zn, predominantly through the appearance of sulfhydryl forms, and we will explore this aspect through XAS analysis in section 3.4.

3.2 Zn concentration in plant biomass and soil

Zinc concentrations in shoots, roots and bulk and rhizopheric soil at the end of the 6 week-growth experiment are presented in Fig. 2. As expected, negligible Zn was detected in plant tissues and soils from the control treatments, consistent with the low Zn content of the topsoil. Zn concentrations were higher in shoots than in the respective roots of all Zn treatments (Fig. 2a-b). Inoculation with *R. leguminosarum* and Zn exposure each had significant effects on shoot Zn concentration (GLM: r^2 (adjusted) = 99.7%, p <0.001 both factors), with shoot Zn concentration greater in the bacterial inoculation than the uninoculated ZnS treatments (Fig. 2a). Shoot Zn concentration was significantly different between all of the Zn treatments and was in the order: $ZnSO_4$ > ZnS > no Zn control. The

300 GLM showed a significant interaction effect on shoot Zn concentrations between bacterial
301 inoculation and Zn exposure (p = 0.003). In conjunction with Fig. 2a, this indicates that
302 bacterial inoculation increased shoot Zn concentrations more in the Zn-exposed treatments
303 than in the control, where the potential for Zn uptake in plant tissues is limited due to the low
304 Zn content of the topsoil. Root Zn concentrations were more variable between duplicate
305 bulked samples for the Zn treatments (Fig. 2b), attributed to the small masses digested for
306 some samples reducing data reliability. Consequently there was no significant detectable
307 effect of bacterial inoculation, Zn exposure or their interaction on root Zn concentration
308 (GLM: r^2 (adjusted) = 15.6%, p >0.05 both factors and their interaction).
309
310 Figure 2 here
311
312 The concentration of Zn was analysed separately in bulk and rhizospheric soils following
313 plant harvest (Fig. 2c). Soil Zn concentrations at the end of the experiment in the Zn-
314 amended treatments (mean values 233-502 mg kg^{-1}) were lower than the initial Zn content
315 (600 mg kg^{-1}), mainly attributed to leaching rather than Zn uptake by *B. juncea* which was
316 estimated at 1-5 mg Zn per pot at the end of the experiment. The three factors tested in the
317 GLM - soil type (bulk vs. rhizospheric), bacterial inoculation and Zn exposure - each had a
318 significant effect on soil Zn concentration (GLM: r^2 (adjusted) = 99.7%, p = 0.016, 0.012 and
319 <0.001, respectively). Zinc concentrations were significantly higher in the rhizospheric
320 compared to the bulk soil and in the bacterial inoculation than in the uninoculated treatments.
321 Soil Zn concentrations were significantly higher in the Zn-amended soils than in the
322 uncontaminated control, but were not significantly different between the $ZnSO_4$ and ZnS
323 treatments. The GLM showed significant interaction effects on soil Zn concentration between
324 the factors bacterial inoculation and soil type (p = 0.005) and between all three factors (Zn

exposure, bacterial inoculation and soil type, $p = 0.005$). In conjunction with Fig. 2c, this was interpreted as indicating that in the Zn exposure treatments, bacterial inoculation results in decreased Zn concentrations in bulk soil and higher Zn concentrations in rhizospheric soil, i.e. a transfer of soil Zn occurs from the bulk soil to rhizospheric soil. This soil Zn fractionation effect in response to bacterial inoculation did not occur in the control treatments due to the low Zn content of the topsoil.

R. leguminosarum is a known rhizosphere bacteria associated with leguminous plants (Adediran et al., 2015; Glick, 1995; Reeve et al., 2010), eliciting growth promotion in plants. Hence, inoculated plants showed some recovery in plant height and root length growth parameters, despite higher tissue Zn concentrations, suggesting that bacteria alleviated the inhibitory effects caused by Zn on plant growth. Most studies interpret such effects as being mediated by synthesis of phytohormones (Brigido and Glick, 2015; Goswami et al., 2016), including indole acetic acid (IAA) (Spaepen and Vanderleyden, 2011) and 1-aminocyclopropane-1-carboxylate (ACC) deaminase (Annapurna et al., 2016; Glick et al., 2007), which alter plant metabolism resulting in healthier plants (Adediran et al., 2015; Ma et al., 2015a,b). However, our data show that shoot tissue Zn concentrations were higher in inoculated plants (Fig. 2a), possibly due to bacterially enhanced solubilisation of Zn through production of siderophores and other metal-chelating substances (Verma et al., 2010). We have previously attributed this apparent paradox of healthy plant growth and increased Zn accumulation to bacterially-mediated changes in Zn speciation, including through complexation with histidine (Adediran et al., 2016b; Medas et al., 2019; Yadav, 2010), organic acids and thiols (Adediran et al., 2015, 2016a; Adele et al., 2018; Grill et al., 1985). Although plants naturally produce these metal detoxification ligands even in the absence of bacterial inoculation (e.g. Kuhnlenz et al., 2016), complexation with them is expected to be

consistently higher in plant tissues in inoculated treatments, particularly in the presence of the more toxic $ZnSO_4$ species. Moreover, in our experiment we note that rhizospheric soil has higher Zn concentration in the bacteria inoculation treatments, especially when plants are challenged with ZnS (Fig. 2c, different lowercase letters for Zn concentrations in the rhizospheric soil between the uninoculated and inoculated ZnS treatments). This suggests that bacteria also elicit accumulation of Zn around plant roots, which may help to drive Zn into roots via diffusional gradients. Finally, our result is in agreement with the observation of Whiting et al. (2001) who reported less Zn accumulation in a Zn hyperaccumulating plant species grown in ZnS-enriched soil than soil amended with other Zn forms (Zn sulfate, Zn phosphate and Zn oxide). Although their ZnS was not in nanoparticulate form, the aggregation observed in our prepared ZnS nanoparticles suggests a similar bioavailability mechanism.

3.3 Soil pH

Soil pH has a dominant effect on solubility, availability and phytotoxicity of metals (Rengel, 2015), by controlling the speciation of metals in soil (Alloway, 1995). The secretion of protons and exudates, including organic acids, by plant roots or microbes may contribute to greater acidity of the rhizosphere (Hinsinger et al., 2009; Zeng et al., 2018) relative to the bulk soil, by amounts that are dependent on plant species and soil factors (Marschner, 1995). An increased rhizosphere acidity will also increase metal solubility and eventually metal accumulation in plants (Li et al., 2010). For a typical *Brassica* species, the optimal soil pH for growth is 6.5 (Zaurov et al., 1999). Thus, to help identify the possible mechanism by which bacteria mobilise Zn from the bulk soil, pHs of rhizospheric and bulk soils measured separately after plant harvest are compared (Table 1).

375 Table 1 here

376

377 Bulk soil pH increased in all treatments between the start and end of the experiment, with the
378 smaller changes in bulk soil pH in the Zn-amended due to buffering through zinc hydrolysis
379 which generates protons. After plant harvest, the rhizospheric soils were significantly (paired
380 t-test, $p = 0.008$) more acidic than bulk soils by 0.09-0.39 pH units within each treatment.
381 Whilst the differences in pH between bulk and rhizospheric soils at the end of the experiment
382 were generally small, in the Zn-exposed soils the magnitude of pH decrease was
383 approximately double in the inoculated treatments compared to the uninoculated treatments.
384 This suggests that soil pH changes in the rhizosphere provide an additional mechanism by
385 which bacteria increase Zn bioavailability to plant roots, although the mechanism driving pH
386 changes was not resolved in our study.

387

388 **3.4 XAS analysis of Zn speciation and distribution in roots and bulk and rhizospheric**
389 **soils**

390

391 XAS was employed to investigate Zn speciation in the bulk soil, the rhizospheric soil and the
392 roots of *B. juncea* grown in soil amended with the Zn treatments 6 weeks after planting. Zinc
393 K-edge XANES spectra and the Zn composition revealed from LCF for roots, bulk and
394 rhizospheric soils are shown for the ZnS nanoparticles treatments in Fig. 3 and for the $ZnSO_4$
395 treatments in Fig. 4.

396

397 In the ZnS nanoparticles treatments (Fig. 3), Zn in the bulk and rhizospheric soils occurred
398 predominantly as ZnS in both the uninoculated and inoculated treatments, ranging from 78 to
399 92%, showing that only a small fraction of the applied ZnS nanoparticles was transformed in

400 the soil during the 6-week growth experiment, partly due to their tendency to aggregate,
401 resulitng in reduced surface energy and solubility (Eskelsen et al., 2018). The remainder was
402 associated with cysteine (1-12%, apart from bulk soil in the uninoculated treatment), phytate
403 (5-8%), sulfate (~3% in the uninoculated treatments only) and polygalacturonate (5%, only in
404 bulk soil in the inoculated treatment). In contrast, the speciation of Zn in the roots in the ZnS
405 treatments was markedly different from that in the soils. In the uninoculated treatment, the
406 fraction of Zn occurring in the roots as ZnS was much lower (45%) and the remaining root
407 Zn was associated with phytate (33%), citrate (16%) and sulfate (7%) (Fig. 3d). In the
408 inoculated ZnS treatment, ZnS was not apparent in root material, with root Zn predominantly
409 associated with phytate (37%), cysteine (31%) and citrate (28%), and also formate (4%), but
410 Zn sulfate was absent (Fig. 3h).
411
412 The predominance of ZnS nanoparticles in bulk and rhizospheric soils is entirely consistent
413 with the low solubility of ZnS in water (~10^{-9} molar based on compilations of Zn salt
414 solubility data (Clever et al., 1992) at the circumneutral pH measured in soils at the end of the
415 experiment). Nevertheless, the presence of other species, namely Zn phytate, Zn cysteine and
416 Zn sulfate, is evidence of some dissolution-mediated transformations. In principle, the
417 production of root exudates should acidify the rhizosphere and help to solubilise Zn
418 (Dessureault-Rompré et al., 2008), although the measured reduction in pH in the rhizospheric
419 compared to the bulk soil during the experiment was small in the ZnS treatments (≤ 0.2 pH
420 units, Table 1). These small changes also imply that oxidative dissolution (which can
421 promote faster acidification) was minimal, although the presence of Zn sulfate in soils and
422 root materials in the uninoculated ZnS treatment indicates the occurrence of this mechanism
423 (Fig. 3d), and other studies have reported the oxidative dissolution of ZnS by plants (Panfili
424 et al., 2005; Voegelin et al., 2011). Finally, the presence of ZnS in roots in the uninoculated

425 treatment indicates that plants can take up metals in both soluble and nanoparticulate forms,
426 consistent with previous studies (e.g. Adele et al., 2018; Lin et al., 2008; Lv et al., 2015).
427
428 The transition from rhizospheric soil to plant root tissue was characterised by a marked drop
429 in the proportion of ZnS (from 78 to 45% and 92 to 0% in the uninoculated and inoculated
430 treatments, respectively), accompanied by a steep increase in Zn phytate and the appearance
431 of Zn citrate. A notable difference between the ZnS inoculated and uninoculated treatments
432 was the presence of Zn formate in roots in the inoculated treatment. Formate accumulation in
433 plant roots has previously been attributed as a response to aluminium and pH stress (Lou et
434 al., 2016). Similarly, Zn phyate and Zn citrate are known major species in plant tissues
435 growing in Zn-contaminated environments (Kopittke et al., 2011; Salt et al., 1999).
436
437 Figure 3 here
438
439 The XANES spectra for bulk and rhizospheric soils and roots of *B. juncea* grown in $ZnSO_4$-
440 amended soil (Fig. 4) differed from those for the ZnS nanoparticle treatments, most notably
441 in the appearance of Zn histidine in all soil and root samples in the $ZnSO_4$ treatments. As in
442 the ZnS treatments, the Zn speciation in bulk and rhizospheric soil samples in both
443 uninoculated and inoculated $ZnSO_4$ treatments was similar, though it was dominated instead
444 by Zn carbonate (22-40%), with the remaining Zn in the form of sulfate (20-29%), histidine
445 (18-27%) and phytate (14-20%). Similarly, Zn speciation in roots in the $ZnSO_4$ treatments
446 differed markedly from that in the soils, particularly in the inoculated treatment. The best
447 LCF fit for uninoculated roots showed Zn was in the form of histidine (38%) > carbonate
448 (24%) > citrate (18%) > phytate (16%) (Fig. 4d), while root Zn in the inoculated treatment
449 was associated (to 2 significant figures) with histidine (64%), cysteine (14%), formate (13%)

450 and oxalate (11%) (Fig. 4h). As with the ZnS treatments, Zn formate appeared in plant roots
451 in the inoculated treatment (Fig. 4h).
452
453 A steep increase in the proportion of Zn histidine between the rhizospheric soil and the root
454 tissue was observed in both uninoculated and inoculated $ZnSO_4$ treatments. The higher
455 proportions of secondary species (other than $ZnSO_4$) reflects the greater solubility of $ZnSO_4$
456 compared to ZnS, allowing the dissolved Zn to complex with other ligands. In particular, the
457 high proportion of Zn carbonate likely reflects the high affinity of Zn for elevated dissolved
458 CO_2 driven by plant root respiration as well as microbial metabolism (Perdrial et al., 2015).
459 On the other hand, the absence of ZnS in the $ZnSO_4$ treatments indicates that the soil did not
460 attain sufficiently reducing conditions to induce sulfate reduction in the 6-week growth
461 period, although this is unlikely given the relatively low organic matter content of the
462 experimental soil (15%), even if sulfate reducing bacteria were present.
463
464 Figure 4 here
465
466 The most significant changes in Zn speciation, in both ZnS and $ZnSO_4$ treatments, occurred
467 between the rhizospheric soil and the root and generally involved an increase in the
468 proportion of Zn associated with organic acids and thiols. In the ZnS treatments, the main
469 organic acid species occurring in roots were Zn phytate and Zn citrate, with Zn formate
470 appearing in the inoculated treatment. In the $ZnSO_4$ treatments, organic acid complexation of
471 Zn in roots was dominated by histidine and citrate in the uninoculated treatment, with the
472 appearance of Zn associated with formate, cysteine and oxalate in the inoculated treatment,
473 but the disappearance of Zn citrate. The most prominent similarity in Zn speciation in roots
474 from the $ZnSO_4$- and ZnS nanoparticles-amended soils was the presence of Zn formate in the

475 bacterial inoculated treatments. Formate accumulation in plant roots has previously been
476 attributed as a response to toxic metal stress (Lou et al., 2016).
477
478 Phytate, also called myoinositol hexakisphosphate, is the most abundant organic phosphate
479 species in soils (Turner et al., 2012), originating from plant residues and animal manure
480 (Annunziata, 2007). Thus, the presence of Zn phytate in the bulk and rhizospheric soil
481 implies either the presence of organic phosphorus in soil or a long range diffusive influence
482 of plant roots. Based on the observed increase in the proportion of Zn associated with phytate
483 between rhizosphere and roots in the ZnS treatments, and the relatively low organic matter
484 content of the experimental soil, we infer the latter is the more likely control on Zn phytate
485 distribution across the different compartments. Indeed, the formation of Zn phytate is a well-
486 known process for Zn immobilisation in roots, possibly as a detoxification mechanism
487 (Adediran et al., 2015; Adele et al., 2018; Kopittke et al., 2011; Terzano et al., 2008; Van
488 Steveninck et al., 1994).
489
490 Citrate is an important organic anion secreted by plant roots as a mechanism for nutrient
491 acquisition from soil, especially under phosphate-deficient conditions (e.g. Jones, 1998;
492 Pearse et al., 2007), as in the experimental soil (0.31 mg g^{-1} P). In our study, citrate appeared
493 as a significant Zn ligand within plant roots but not in soil samples, indicating that, unlike
494 phytate, it does not appear to have a long range diffusive influence in the bulk soil. Although
495 one study ruled out organic acid complexation of Zn in root tissue (Medas et al., 2015),
496 citrate complexation has been estimated to account for 30% of Zn occurring in rhizosphere
497 solution (Dessureault-Rompré et al., 2008), and citrate binding of metals has been identified
498 in other plant tissues, including Zn in shoots of *Thlaspi caerulescens* (Salt et al., 1999).
499

Histidine is an essential amino acid with a positively charged imidazole functional group (Chakrabarti, 1990; Gluster, 1991; Gramlich et al., 2013). The occurrence of Zn histidine in the roots in the $ZnSO_4$ treatments in the present study agrees with previous studies of Zn hyperaccumulator species (Adediran et al., 2016b; Lasat et al., 1998; Salt et al., 1999). Metal tolerance and hyperaccumulation via histidine complexation has been demonstrated in studies involving Ni (Salt et al. 1999) and histidine has been implicated in Cu and Zn toxicity responses (Sharma and Dietz, 2006). Salt et al. (1999) showed that histidine was part of the root exudate pool produced as a response to Ni exposure that led to increased Ni concentrations in both accumulating and non-accumulating species of *Thlaspi caerulescens*. In our study, Zn histidine was only detected in $ZnSO_4$ treatments with similar gradients across the bulk soil to rhizosphere to roots between inoculated and uninoculated treatments. We found higher proportions of Zn histidine complexes in roots than in the bulk and rhizospheric soils, where the proportions were approximately equal. Therefore, like phytate, we interpret the observed gradient as reflecting histidine production in the form of root exudates (see also Adediran et al., 2016b) but with long range transport into the rhizospheric and bulk soil.

Finally, this study confirms the importance of Zn cysteine complexation in roots of bacteria inoculated plants challenged with ZnS and $ZnSO_4$, as reported previously for $ZnSO_4$ (Adediran et al., 2015, 2016a; Adele et al., 2018), and further that the transformation occurs within the plant (epidermal) tissue and not in the rhizoplane (Adediran et al., 2016a). The formation of cysteine in roots of plants is closely linked to sulfate metabolism, in which sulfate is first converted to sulfide, which combines with *O*-acetylserine to form cysteine (Adediran et al., 2016a; Leustek, 2002; Leustek and Saito 1999). The limited occurrence of Zn cysteine complexes in compartments of the uninoculated ZnS treatment, alongside the

presence of Zn sulfate suggests that the inoculated bacteria play a role in triggering formation of cysteine from sulfate.

Conclusions

We hypothesised that the rhizosphere should be a zone of active changes in metal speciation during growth of plants in metal-contaminated soils, and that bacteria exert a primary control on the type of metal species formed. We used *B. juncea* growing in Zn-contaminated soil with and without bacterial inoculation to test our hypotheses, employing XAS to determine Zn speciation in bulk soil, rhizospheric soil and roots. Broadly, we found that: (i) within the soil (bulk and rhizospheric) environment, speciation depended on the form in which Zn was introduced to the soil (ZnS vs. $ZnSO_4$), (ii) Zn speciation in the root was dominated by organic acids (phytate, citrate and histidine) and thiols (cysteine), and (iii) bacteria enhanced transformations across the rhizosphere towards organic acid and thiol complexation of Zn in the root. Differences in Zn speciation between $ZnSO_4$ and ZnS nanoparticles treatments in the rhizosphere-root interface indicate different uptake mechanisms of different Zn forms by *B. juncea*. Our investigation suggested that *R. leguminosarum* induced speciation changes across the rhizosphere and plant root depending on the form of Zn in soil. These mechanisms have direct implications for the speciation and mobility of Zn in Zn-contaminated soil. Thus, this study clearly indicates that Zn form is a strong factor influencing its speciation in the rhizosphere-root interface, rather than the total Zn concentration in soil. XAS analysis enables the speciation of Zn to be determined at the low concentrations often prevalent in plant tissues, aiding the understanding of fate of Zn in both the soil and plant.

Acknowledgements

The authors are grateful for the financial support of the Rivers-State Sustainable Development Agency, Nigeria, and the Diamond Light Source, UK, for providing synchrotron beamtime through grant SP10429. The support of staff in the laboratories and glasshouses at the University of Edinburgh is also acknowledged.

Supplementary Material. Characterisation of the experimental soil (S1). Details of plant growth experiment materials, set-up and conduct (S2). Details of X-ray absorption spectroscopy studies on soils and plant roots (S3).

References

Adediran, G.A., Ngwenya, B.T., Mosselmans, J.F.W., Heal, K.V., Harvie, B.A., 2015. Mechanisms behind bacteria induced plant growth promotion and Zn accumulation in *Brassica juncea.* Journal of Hazardous Materials **283**, 490–499.

Adediran, G.A., Ngwenya, B.T., Mosselmans, J.F.W., Heal, K.V., 2016a. Bacteria-zinc co-localization implicates enhanced synthesis of cysteine-rich peptides in zinc detoxification when *Brassica juncea* is inoculated with *Rhizobium leguminosarum*. New Phytologist **209**, 280–293.

Adediran, G.A., Ngwenya, B.T., Mosselmans, J.F.W., Heal, K.V., Harvie, B.A., 2016b. Mixed planting with a leguminous plant outperforms bacteria in promoting growth of a metal remediating plant through histidine synthesis. International Journal of Phytoremediation **18,** 720–729.

Adele, N. C., Ngwenya, B.T., Heal, K. V., Mosselmans J. F. W., 2018. Soil bacteria override speciation effects on zinc phytotoxicity in zinc-contaminated soils. Environmental Science & Technology **52***,* 3412–3421.

Allen, S.E., Grimshaw, H.M., Parkinson, J.A., Quarmby, C.L., 1974. Chemical Analysis of Ecological Materials*.* Blackwell Scientific Publications, Oxford.

Alloway, B., 1995. Heavy Metals in Soils. Chapman and Hall, London.

Annapurna, D., Rajkumar, M., Prasad, M.N.V., 2016. Potential of castor bean (*Ricinus communis* L.) for phytoremediation of metalliferous waste assisted by plant growth-promoting bacteria: possible cogeneration of economic products, in: Prasad, M.N.V. (Ed.), Bioremediation and Bioeconomy. Elsevier, Amsterdam, pp. 149–175.

Annunziata, M.F., 2007. Origin and biochemical transformations of inositol stereoisomers and their phosphorylated derivatives in soil, in: Turner B.L., Richardson A.E., Mullaney E.J., (Eds.), Inositol Phosphates: Linking Agriculture and the Environment. CABI, Wallingford, United Kingdom, pp. 41–60.

Auffan, M., Rose, J., Bottero, J.Y., Lowry, G.V., Jolivet, J.P., Wiesner, M.R., 2009. Towards a definition of inorganic nanoparticles from an environmental, health and safety perspective. Nature Nanotechnology **4,** 634–641.

Bardgett, R.D., van der Putten, W.H., 2014. Belowground biodiversity and ecosystem functioning. Nature **515**, 505–511.

Bhattacharjee, H., Rosen, B.P., 2007. Arsenic metabolism in Prokaryotic and Eukaryotic Microbes, in: Nies, D.H., Silver, S. (Eds.), Molecular Microbiology of Heavy Metals, Microbiology Monographs, Volume 6. Springer, Berlin, pp. 371–406.

Biruntha, M., Archana, J., Kavitha, K., Selvi, B.K., Paul, J.A.J., Balachandar, R., Saravana, M., Karmegan, N., 2020. Green synthesis of zinc sulfide nanoparticles using *Abrus precatorius* and its effect on coelomic fluid protein profile and enzymatic activity of the earthworm, *Eudrilus eugeniae*. BioNanoScience **10**, 149–156.

Bishnoi, U., 2015. PGPR interaction: an ecofriendly approach promoting the sustainable agriculture system, in: Basis, H., Sherrier, J. (Eds.), Plant Microbe Interactions, Advances in Botanical Research **75**. Academic Press, London, pp. 81–113.

Boi, M.E., Medas, D., Aquilanti, G., Bacchetta, G., Birarda, G., Cappai, G., Carlomagno, I., Casu, M.A., Gianoncelli, A., Meneghini, C., Piredda, M., Podda, F., Porceddu, M., Rimondi, V., Vaccari, L., De Giudici, G., 2020. Mineralogy and Zn chemical speciation in a soil-plant system from a metal-extreme environment: A study on *Helichrysum microphyllum* subsp. *tyrrhenicum* (Campo Pisano Mine, SW Sardinia, Italy). Minerals **10**, 259.

Brígido, C., Glick B.R., 2015. Phytoremediation Using Rhizobia, in: Ansari A.A., Gill S.S., Gill R., Lanza G.R., Newman L. (Eds.), Phytoremediation, Management of Environmental Contaminants, Volume 2. Springer Cham, Heidelberg, pp. 95–114.

Broadley, M.R., White, P.J., Hammond, J.P., Zelko, I., Lux, A., 2007. Zinc in plants. New Phytologist **173,** 677–702.

Buée, M., De Boer, W., Martin, F., van Overbeek, L., Jurkevitch, E., 2009. The rhizosphere zoo: An overview of plant-associated communities of microorganisms, including phages, bacteria, archaea, and fungi, and of some of their structuring factors. Plant and Soil **321**, 189–212.

Chakrabarti, P., 1990. Geometry of interaction of metal ions with histidine residues in protein structures. Protein Engineering **4,** 57–63.

Chandrangsu, P., Rensing, C., Helmann, J.D., 2017. Metal homeostasis and resistance in bacteria. Nature Reviews Microbiology **15**, 338–350.

Chiang, K.Y., Wang, Y.N., Wang, M.K., Chiang, P.N., 2006. Low-molecular-weight organic acids and metal speciation in rhizosphere and bulk soils of a temperate rain forest in Chitou, Taiwan. Taiwan Journal of Forest Science **21**, 327–337.

Clever, H.L., Derrick, M.E., Johnson, S.A., 1992. The solubility of some sparingly soluble salts of zinc and cadmium in water and in aqueous-electrolyte solutions. Journal of Physical and Chemical Reference Data **21,** 941–1004.

Dessureault-Rompré, J., Nowack, B., Schulin, R., Tercier-Waeber, M.L., Luster, J., 2008. Metal solubility and speciation in the rhizosphere of *Lupinus albus* cluster roots. Environmental Science & Technology **42,** 7146–7151.

Eskelsen, J.R., Xu, J., Chiu, M., Moon, J-W., Wilkins, B., Graham, D.E., Gu, B., Pierce, E.M., 2018. Influence of structural defects on biomineralized ZnS nanoparticle dissolution: An in-situ electron microscopy sudy. Environmental Science & Technology 52 (3), 1139-1149.

Fang, X., Zhai, T., Gautam, U.K., Li, L., Wu, L., Bando, Y., Golberg, D., 2011. ZnS nanostructures: From synthesis to applications. Progress in Materials Science **56**, 175–287.

Feldmann, J., Bluemlein, K., Krupp, E.M, Mueller, M., Wood, B.A., 2018. Metallomics study in plants exposed to arsenic, mercury, selenium and sulphur, in: Arruda, M.A.Z. (Ed.) Metallomics: The Science of Biometals, Advances in Experimental Medicine and Biology, Volume 1055. Springer International, Cham, Switzerland, pp. 67–100.

Gadd, G.M., 2010. Metals, minerals and microbes: geomicrobiology and bioremediation Microbiology **156,** 609–643.

Ganguly, S., Das, S., Dastidar, S.G., 2014. Study of antimicrobial effects of the anticancer drug oxaliplatin and its interaction with synthesized ZnS nanoparticles. International Journal of Pharmacy and Therapeutics **5,** 230–234.

Glick, B.R., 1995. The enhancement of plant growth by free-living bacteria. Canadian Journal of Microbiology **41,** 109–117.

Glick, B.R., 2014. Bacteria with ACC deaminase can promote plant growth and help to feed the world. Microbiological Research **169,** 30–39.

Glick, B.R., Cheng, Z., Czarny, J., Duan, J., 2007. Promotion of plant growth by ACC deaminase-producing soil bacteria. European Journal of Plant Pathology **119,** 329–339.

Glusker, J.P., 1991. Structural aspects of metal liganding to functional groups in proteins, in: Anfinsen, C.B., Edsall, J.T., Richards, F.M., Eisenberg, D.S. (Eds.), Metalloproteins: Structural Aspects, Advances in Protein Chemistry, Volume 42. Academic Press, London, pp. 1–76.

Goswami, D., Thakker, J.N., Dhandhukia, P.C., 2016. Portraying mechanics of plant growth promoting rhizobacteria (PGPR): a review. Cogent Food and Agriculture **2,** 1–19.

Gramlich, A., Tandy, S., Frossard, E., Eikenberg, J., Schulin, R., 2013. Availability of zinc and the ligands citrate and histidine to wheat: does uptake of entire complexes play a role? Journal of Agricultural and Food Chemistry **61,** 10409–10417.

Grill, E., Winnacker, E.L., Zenk, M.H., 1985. Phytochelatins: the principal heavy metal complexing peptides of higher plants. Science **230,** 674–676.

Guo, D., Fan, Z., Lu, S., Ma, Y., Nie, X., Tong, F., Peng, X., 2019. Changes in rhizosphere bacterial communities during remediation of heavy metal-accumulating plants around the Xikuangshan mine in southern China. Scientific Reports **9,** 1947.

Helliwell, J. R., Sturrock, C. J., Mairhofer, S., Craigon, J., Ashton, R. W., Miller, A. J., Whalley, W. R., Mooney, S. J., 2017. The emergent rhizosphere: imaging the development of the porous architecture at the root-soil interface. Scientific Reports **7**, 14875.

Hernandez-Viezcas, J.A., Castillo-Michel, H., Servin, A.D., Peralta-Videa, J.R., Gardea-Torresdey, J.L., 2011. Spectroscopic verification of zinc absorption and distribution in the desert plant *Prosopis juliflora-velutina* (velvet mesquite) treated with ZnO nanoparticles. Chemical Engineering Journal **170,** 346–352.

Hinsinger, P., Bengough, A.G., Vetterlein, D., Young, I.M., 2009. Rhizosphere: biophysics, biogeochemistry and ecological relevance. Plant and Soil **321**, 117–152.

Jambon, I., Thijs, S., Weyens, N., Vangronsveld, J., 2018. Harnessing plant-bacteria-fungi interactions to improve plant growth and degradation of organic pollutants. Journal of Plant Interactions **13**, 119–130.

Jilling, A., Keiluweit, M., Contosta, A.R., Frey, S., Schimel, J., Schnecker, J., Smith, R.G., Tiemann, L., Grandy, A.S., 2018. Minerals in the rhizosphere: Overlooked mediators of soil nitrogen availability to plants and microbes. Biogeochemistry **139,** 103–122.

Jones, D.L., 1998. Organic acids in the rhizosphere - a critical review. Plant and Soil **205,** 25–44.

Khan, A.A., Ellis, D.R., Huang, X., Norton, G.J., Meharg, A.A., Salt, D.E., Csonka L.N., 2018. Glutathione-S-transferase from the arsenic hyperaccumulator fern *Pteris vittata* can confer increased arsenate resistance in *Escherichia coli*. BioRxiv https://doi.org/10.1101/379511

Khanna, K., Jamwal, V.L., Gandhi, S.G., Ohri, P., Bhardwaj R., 2019. Metal resistant PGPR lowered Cd uptake and expression of metal transporter genes with improved growth and photosynthetic pigments in *Lycopersicon esculentum* under metal toxicity. Scientific Reports **9,** 5855.

Kim, K.R., Owens, G., Kwon, S.L., 2010. Influence of Indian mustard (*Brassica juncea*) on rhizosphere soil solution chemistry in long-term contaminated soils: a rhizobox study. Journal of Environmental Sciences **22,** 98–105.

Kopittke, P.M. Menzies, N.W., de Jonge, M.D., McKenna, B.A., Donner, E., Webb, R.I., Paterson, D.J., Howard, D.L., Ryan, C.G., Glover, C.J., Scheckel, K.G., Lombi, E. 2011. In situ distribution and speciation of toxic copper, nickel, and zinc in hydrated roots of cowpea. Plant Physiology **156,** 663–673.

Kühnlenz, T., Hofmann, C., Uraguchi, S., Schmidt, H., Schempp, S., Weber, M., Lahner, B., Salt, D.E., Clemens, S., 2016. Phytochelatin synthesis promotes leaf Zn accumulation of *Arabidopsis thaliana* plants grown in soil with adequate Zn supply and is essential for survival on Zn-contaminated soil. Plant and Cell Physiology **57**, 2342–2352.

Lanson, B., Marcus, M.A., Fakra, S., Panfili, F., Geoffroy, N., Manceau, A., 2008. Formation of Zn-Ca phyllomanganate nanoparticles in grass roots. Geochimica et Cosmochimica Acta **72,** 2478–2490.

Lasat, M.M., Baker, A.J., Kochian, L.V., 1998. Altered Zn compartmentation in the root symplasm and stimulated Zn absorption into the leaf as mechanisms involved in Zn hyperaccumulation in *Thlaspi caerulescens*. Plant Physiology **118,** 875–883.

Lee, S., Kim, Y., Kim, J.M., Chu, B., Joa, J., Sang, M.K., Song, J., Weon, H., 2019. A preliminary examination of bacterial, archaeal, and fungal communities inhabiting different rhizocompartments of tomato plants under real-world environments. Scientific Reports **9**, 9300.

Leustek, T., 2002. Sulfate metabolism. The Arabidopsis Book **2002 (1)**, e0017. https://doi.org/10.1199/tab.0017

Leustek T., Saito, K., 1999. Sulfate transport and assimilation in plants. Plant Physiology **120,** 637–643.

Li, W.C., Ye, Z.H., Wong, M.H., 2010. Metal mobilization and production of short-chain organic acids by rhizosphere bacteria associated with a Cd/Zn hyperaccumulating plant, *Sedum alfredii*. Plant and Soil **326**, 453–467.

Lin, D., Xing, B., 2008. Root uptake and phytotoxicity of ZnO nanoparticles. Environmental Science & Technology **42,** 5580–5585.

Lou, H.Q., Gong, Y.L., Fan, W., Xu, J.M., Liu, Y., Cao, M.J., Wang, M.H., Yang, J.L., Zheng, S.J., 2016. A formate dehydrogenase confers tolerance to aluminum and low pH. Plant Physiology **171**, 294–305.

Luo, S.L., Chen L., Chen, J.L., Xiao, X., Xu, T.Y., Wan, Y., Rao, C., Liu, C.B., Liu, Y.T., Lai, C., Zeng, G.M., 2011. Analysis and characterization of cultivable heavy metal-resistant bacterial endophytes isolated from Cd-hyperaccumulator *Solanum nigrum* L. and their potential use for phytoremediation. Chemosphere **85**, 1130–1138.

Lv, J., Zhang, S., Luo, L., Zhang, J., Yang, K., Christie, P., 2015. Accumulation, speciation and uptake pathway of ZnO nanoparticles in maize. Environmental Science Nano **2,** 68–77.

Lv, J., Christie P., Zhang, S., 2019. Uptake, translocation, and transformation of metal-based nanoparticles in plants: recent advances and methodological challenges. Environmental Science Nano **6**, 41–59.

Ma, C., White, J.C., Zhao, J., Zhao, Q., Xing, B., 2018. Uptake of engineered nanoparticles by food crops: characterization, mechanisms, and implications. Annual Review of Food Science & Technology **9,** 129–153.

Ma, Y., Rajkumar, M., Rocha, I., Oliveira, R.S., Freitas, H., 2015a. Serpentine bacteria influence metal translocation and bioconcentration of *Brassica juncea* and *Ricinus communis* grown in multi-metal polluted soils. Frontiers in Plant Science **5,** 757.

Ma, Y., Oliveira, R.S., Wu, L., Luo, Y., Rajkumar, M., Rochas, I., Frietas, H., 2015b. Inoculation with metal mobilizing plant growth promoting rhizobacterium *Bacillus* sp.SC2b and its role in rhizoremediation. Journal of Toxicology and Environmental Health Part A, **78,** 931–944.

Marschner, H., 1995. Mineral Nutrition of Higher Plants. Academic Press, London.

Medas, D., De Giudici, G., Casu, M.A., Musu, E., Gianoncelli, A., Iadecola, A., Meneghini, C., Tamburini, E., Sprocati, A.R., Turnau, K., Lattanzi, P., 2015. Microscopic processes ruling the bioavailability of Zn to roots of *Euphorbia pithyusa* L. Pioneer plant. Environmental Science & Technology **49,** 1400–1408.

Medas, D., De Giudici, G., Pusceddu, C., Casu, M.A., Birarda, G., Vaccari, L., Gianoncelli, A., Meneghini, C., 2019. Impact of Zn excess on biomineralization processes in *Juncus acutus* grown in mine polluted sites. Journal of Hazardous Materials **370**, 98–107.

Mesa, V., Navazas, A., González-Gil, R., González, A., Weyens, N., Lauga, B., Gallego, J.L.R., Sánchez, J., Peláez, A.I., 2017. Use of endophytic and rhizosphere bacteria to improve phytoremediation of arsenic-contaminated industrial soils by autochthonous *Betula celtiberica*. Applied and Environmental Microbiology **83,** e03411–16. https://doi.org/10.1128/AEM.03411-16

Panfili, F., Manceau, A., Sarret, G., Spadini, L., Kirpichtchikova, T., Bert, V., Laboudigue, A., Marcus, M.A., Ahamdach, N., Libert, M.-F., 2005. The effect of phytostabilization on Zn speciation in a dredged contaminated sediment using scanning electron microscopy, X-ray fluorescence, EXAFS spectroscopy, and principal components analysis. Geochimica et Cosmochimica Acta **69,** 2265–2284.

Pearse, S.J., Veneklaas, E.J., Cawthray, G.R., Bolland, M.D.A., Lambers, H., 2007. Carboxylate composition of root exudates does not relate consistently to a crop species' ability to use phosphorus from aluminum, iron or calcium phosphate sources. New Phytologist **173**,181–190.

Perdrial, J., Thompson, A., Chorover, J., 2015. Soil Geochemistry in the Critical Zone: Influence on Atmosphere, Surface- and Groundwater Composition, in: Giardino, J.R., Houser, C. (Eds.), Principles and Dynamics of the Critical Zone, Developments in Earth Surface Processes, Volume 19. Elsevier, Amsterdam, pp.173–201.

Pradas del Real, A.E., Castillo-Michel, H., Kaegi, R., Sinnet, B., Magnin, V., Findling, N., Villanova, J., Carrière, M., Santaella, C., Fernández-Martínez, A., Levard, C., Sarret, G., 2016. Fate of Ag-NPs in sewage sludge after application on agricultural soils. Environmental Science & Technology **50,** 1759–1768.

Qu, J., Luo, C., Cong, Q., Yuan, X., 2012. A new insight into the recycling of hyperaccumulator: synthesis of the mixed Cu and Zn oxide nanoparticles using *Brassica juncea*. International Journal of Phytoremediation **14,** 854–860.

Rascio, N., Navari-Izzo, F., 2011. Heavy metal hyperaccumulating plants: How and why do they do it? And what makes them so interesting? Plant Science **180,** 169–181.

Ravel, B., Newville, M., 2005. Athena, Artemis, Hephaestus: data analysis for X-ray absorption spectroscopy using IFEFFIT. Journal of Synchrotron Radiation **12,** 537–541.

Reeve, W., O'Hara, G., Chain, P., Ardley, J., Bräu, L., Nandesena, K., Tiwari, R., Copeland, A., Nolan, M., Han, C., Brettin, T., Land, M., Ovchinikova, G., Ivanova, N., Mavromatis, K., Markowitz, V., Kyrpides, N., Melino, V., Denton, M., Yates, R., Howieson, J., 2010. Complete genome sequence of *Rhizobium leguminosarum* bv. *trifolii* strain WSM1325, an effective microsymbiont of annual Mediterranean clovers. Standards in Genomic Sciences **2,** 347–356.

Rengel, Z., 2015. Availability of Mn, Zn and Fe in the rhizosphere. Journal of Soil Science and Plant Nutrition **15,** 397–409.

Rico, C.M., Johnson, M. G., Marcus, M. A., 2018. Cerium oxide nanoparticles transformation at the root-soil interface of barley (*Hordeum vulgare* L.). Environmental Science Nano **5,** 1807–1812.

Rizwan, M., Ali, S., Qayyum, M.F., Ok, Y.S., Adrees, M., Ibrahim, M., Zia-ur-Rehman, M., Farid, M., Abbas, F., 2017. Effect of metal and metal oxide nanoparticles on growth and physiology of globally important food crops: A critical review. Journal of Hazardous Materials **322,** 2–16.

Rout, G.R., Das, P., 2009. Effect of metal toxicity on plant growth and metabolism: I. Zinc, in: Lichtfouse, E., Navarrete, M., Debaeke, P., Véronique, S., Alberola, C. (Eds.), Sustainable Agriculture. Springer, Dordrecht, pp. 873–884.

Salt, D.E., Prince, R.C., Baker, A.J.M., Raskin, I., Pickering, I.J., 1999. Zinc ligands in the metal hyperaccumulator *Thlaspi caerulescens* as determined using X-ray absorption spectroscopy. Environmental Science & Technology **33,** 713–717.

Sessitsch, A., Kuffner, M., Kidd, P., Vangronsveld, J., Wenzel, W.W., Fallmann, K., Puschenreiter M., 2013. The role of plant-associated bacteria in the mobilization and phytoextraction of trace elements in contaminated soils. Soil Biology and Biochemistry **60**, 182–194.

Sharma, S.S., Dietz, K.J., 2006. The significance of amino acids and amino acid-derived molecules in plant responses and adaptation to heavy metal stress. Journal of Experimental Botany **57,** 711–726.

Spaepen, S. Vanderleyden, J., 2011. Auxin and Plant-Microbe interactions. Cold Spring Harbor Perspectives in Biology **3(4)**, a001438. doi: 10.1101/cshperspect.a001438

Terzano, R., Al Chami, Z., Vekemans, B., Janssens, K., Miano, T., Ruggiero, P., 2008. Zinc distribution and speciation within rocket plants (*Eruca vesicaria* L. *Cavalieri*) grown on a polluted soil amended with compost as determined by XRF microtomography and micro-XANES. Journal of Agricultural and Food Chemistry **56,** 3222–3231.

Turner, B.L., Cheesman, A.W., Godage, H.Y., Riley, A.M., Potter, B.V., 2012. Determination of *neo*- and D-*chiro*-inositol hexakisphosphate in soils by solution ^{31}P NMR spectroscopy. Environmental Science & Technology **46,** 4994–5002.

Van Steveninck, R.F.M., Babare, A., Fernando, D.R., Van Steveninck, M.E., 1994. The binding of zinc, but not cadmium, by phytic acid in roots of crop plants. Plant and Soil **167,** 157–164.

Verma, J.P., Yadav, J., Tiwari, K.N., 2010. Application of *Rhizobium* sp. BHURC01 and plant growth promoting rhizobactria on nodulation, plant biomass and yields of chickpea (*Cicer arietinum* L.). International Journal of Agricultural Research **5,** 148–156.

Voegelin, A., Jacquat, O., Pfister, S., Barmettler, K., Scheinost, A.C., Kretzschmar, R., 2011. Time-dependent changes of zinc speciation in four soils contaminated with zincite or sphalerite. Environmental Science & Technology **45**, 255–261.

Wang, B., Liu, L., Gao, Y., Chen, J., 2009. Improved phytoremediation of oilseed rape (*Brassica napus*) by *Trichoderma* mutant constructed by restriction enzyme-mediated integration (REMI) in cadmium polluted soil. Chemosphere **74,** 1400–1403.

Whiting, S., Leake, J., McGrath, S., Baker, A., 2001. Zinc accumulation by *Thlaspi caerulescens* from soils with different Zn availability: a pot study. Plant and Soil **236,** 11–18.

Wu, Z., Li, J., Zheng, J., Liu, J., Liu, S., Lin, W., Wu, C., 2017. Soil microbial community structure and catabolic activity are significantly degenerated in successive rotations of Chinese fir plantations**.** Scientific Reports **7**, 6691.

Yadav, S.K., 2010. Heavy metal toxicity in plants: an overview on the role of glutathione and phytochelatins in heavy metal stress tolerance of plants. South African Journal of Botany **76,** 167–179.

Zaurov, D.E., Perdomo, P., Raskin, I., 1999. Optimizing soil fertility and pH to maximize cadmium removed by Indian mustard from contaminated soils. Journal of Plant Nutrition **22,** 977–998.

Zhalnina, K., Louie, K.B., Hao, Z., Mansoori, N., da Rocha, U.N., Shi, S., Cho, H., Karaoz, U., Loqué, D., Bowen, B.P., Firestone, M.K., Northen, T.R., Brodie, E.L., 2018. Dynamic root exudate chemistry and microbial substrate preferences drive patterns in rhizosphere microbial community assembly. Nature Microbiology **3,** 470–480.

Zhang, H.; Chen, B.; Banfield, J. F., 2018. Particle Size and pH Effects on Nanoparticle Dissolution J. Phys. Chem. C, 114 (35) 14876– 14884.

Zhao, L., Huang, Y., Hu, J., Zhou, H., Adeleye, A.S., Keller, A.A., 2016. ^{1}H NMR and GC-MS based metabolomics reveal defense and detoxification mechanism of cucumber plant under nano-Cu stress. Environmental Science & Technology **50,** 2000–2010.

940 **Table 1.** Mean pH (bold) of rhizosphere and bulk soils after 6 weeks growth of *B. juncea* in
941 soils amended with 600 mg of Zn kg^{-1} of different Zn species with and without inoculation
942 with *R. leguminosarum*. Mean pH of the bulk soils after amendment but before seed sowing
943 are also shown. pH values are means of two subsamples of each treatment shown in
944 parentheses.
945
946
947
948
949
950
951
952
953
954
955

Treatment	**Before sowing**	**After 6 weeks plant growth**	
	Bulk soil	**Bulk soil**	**Rhizosphere soil**
Control	**6.25** (6.20, 6.30)	**7.75** (7.75, 7.75)	**7.63** (7.63, 7.63)
Inoculated Control	**6.20** (6.20, 6.20)	**7.55** (7.55, 7.55)	**7.46** (7.46, 7.46)
$ZnSO_4$	**6.51** (6.50, 6.52)	**6.90** (6.90, 6.91)	**6.70** (6.70, 6.71)
Inoculated $ZnSO_4$	**6.50** (6.50, 6.50)	**6.81** (6.81, 6.81)	**6.42** (6.43, 6.42)
ZnS	**7.45** (7.45, 7.45)	**7.64** (7.65, 7.64)	**7.52** (7.52, 7.52)
Inoculated ZnS	**7.46** (7.46, 7.46)	**7.62** (7.62, 7.61)	**7.42** (7.42, 7.41)

Fig. 1. Measures of growth of *B. juncea* in uninoculated and inoculated with *R. leguminosarum* treatments 6 weeks after planting in uncontaminated (control) and Zn-contaminated (600 mg Zn kg^{-1}) topsoil: (a) plant height, (b) root length, (c) shoot dry biomass, (d) root dry biomass. Values are means of three pots and error bars are standard error. Note different y-axis scales. Different lowercase letters above the bars indicate significant differences in the growth measure between treatments (p <0.05, following Tukey multiple comparison tests in the GLMs).

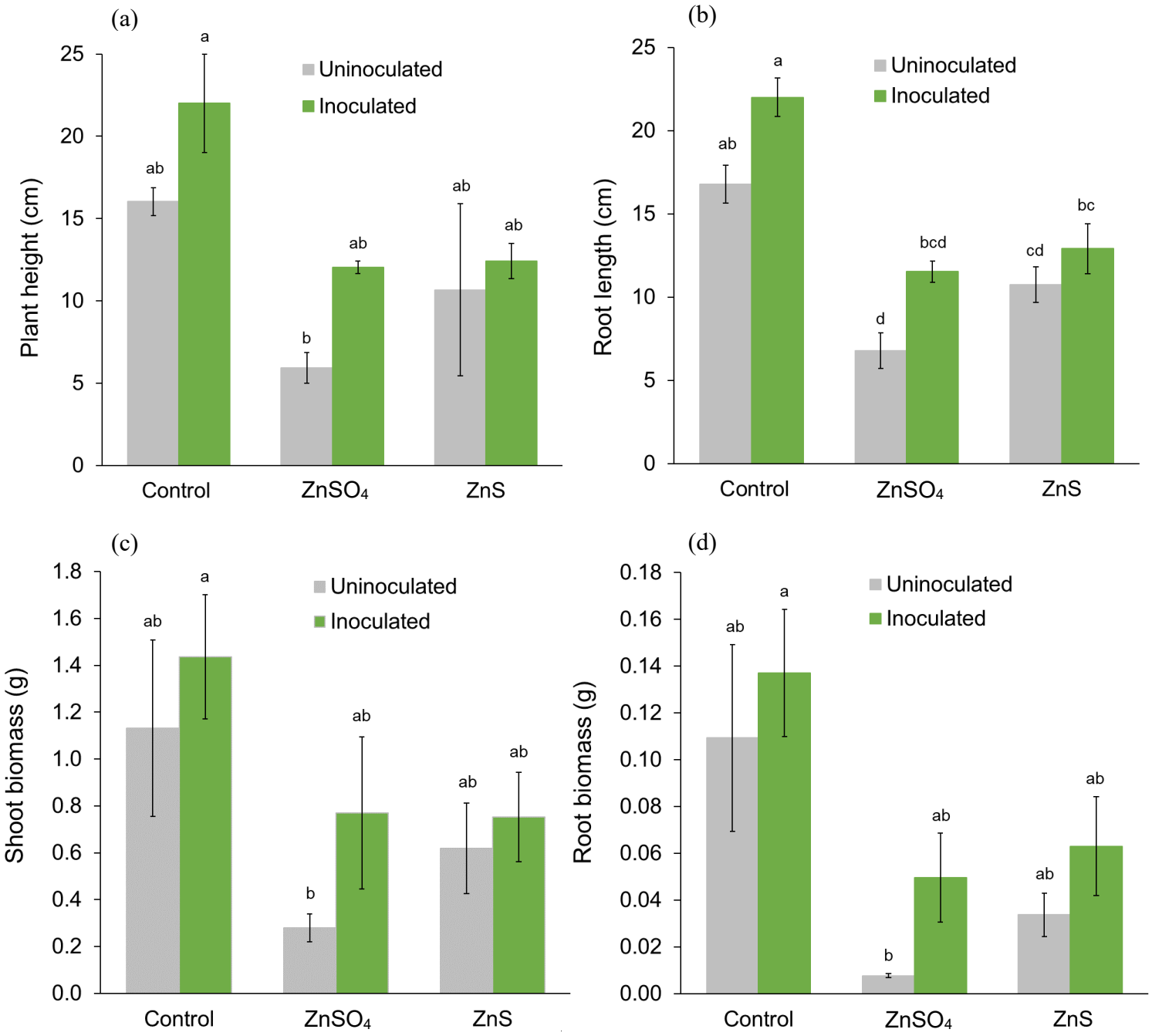

Fig. 2. Zn concentrations in *B. juncea* (a) shoot biomass, (b) root biomass and (c) bulk and rhizosphere soil, 6 weeks after planting in uncontaminated (control) and Zn-contaminated (600 mg Zn kg^{-1}) topsoil in uninoculated and inoculated with *R. leguminosarum* treatments. Values are means of duplicate subsamples composited across all three pots for each treatment, and error bars are standard error. Different lowercase letters above the bars indicate significant differences in Zn concentration between treatments (p <0.05, following Tukey multiple comparison tests in the GLMs). No letters are shown in (b) as there was no significant difference in root Zn concentration between treatments.

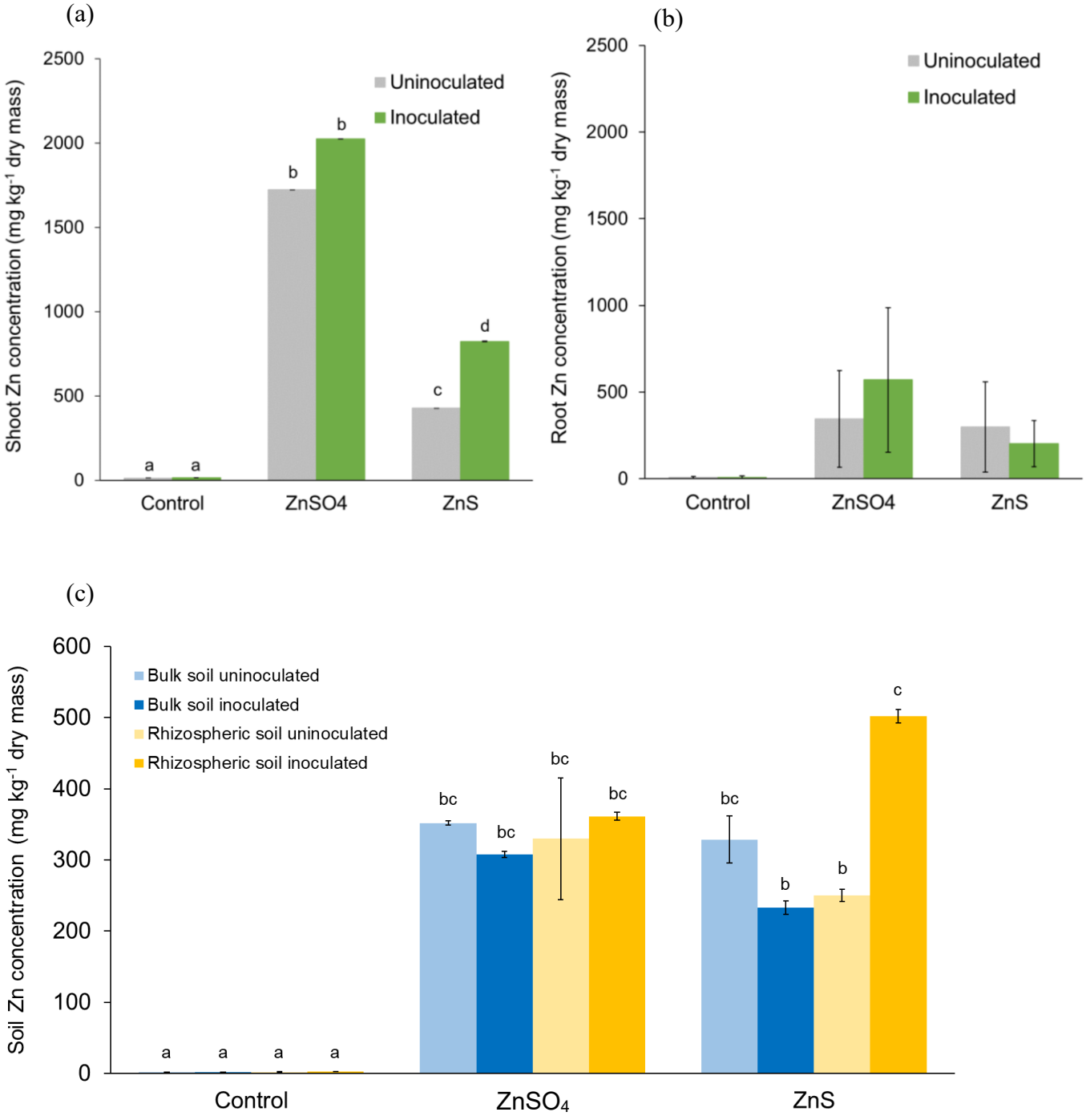

Fig. 3. Zinc speciation results from XAS for *B. juncea* exposed to 600 mg kg^{-1} ZnS nanoparticles in uninoculated treatments (upper row) and inoculated treatments (lower row). Zn K-edge XANES spectra for bulk soil (a, e), rhizospheric soil (b, f) and root (c, g) samples. XANES spectra for each sample and its LCF model fit are the blue and red lines, respectively. *R*-factor shown for each LCF fit. Where duplicate samples were analysed (b, c, f, g), spectra and *R*-factor are shown for one replicate. Zn compound composition (%) of bulk soil, rhizospheric soil and soil obtained from LCF (d, h). ZnS, ZnS nanoparticles; ZnPhy, Zn phytate; $ZnSO_4$, Zn sulfate; ZnCys, Zn cysteine; ZnCit, Zn citrate; ZnForm, Zn formate; ZnPGA, Zn polygalacturonate. Error bars are standard error of duplicate rhizospheric soil and root samples analysed in inoculated and uninoculated treatments.

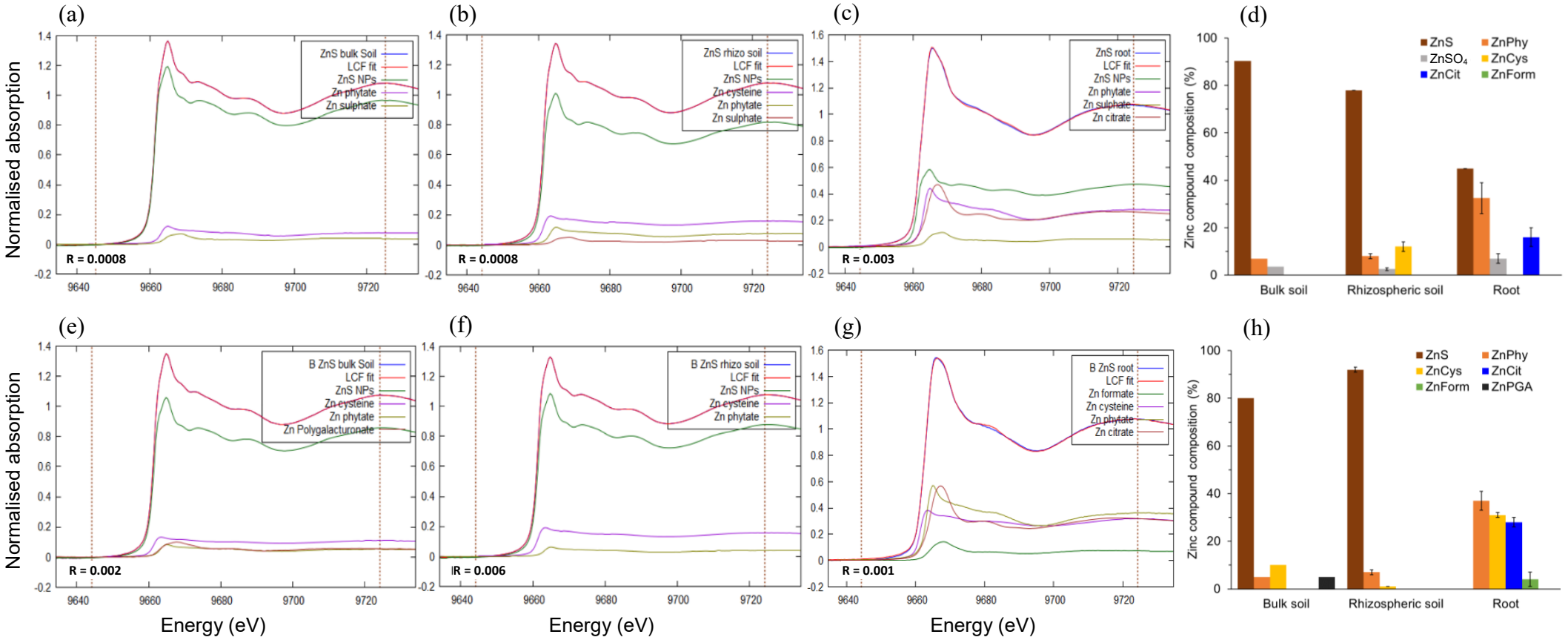

Fig. 4. Zinc speciation results from XAS for *B. juncea* exposed to 600 mg kg^{-1} $ZnSO_4$ in uninoculated treatments (upper row) and inoculated treatments (lower row). Zn K-edge XANES spectra for bulk soil (a, e), rhizospheric soil (b, f) and root (c, g) samples. XANES spectra for each sample and its LCF model fit are the blue and red lines, respectively. *R*-factor shown for each LCF fit. Where duplicate samples were analysed (f, g), spectra and *R*-factor are shown for one replicate. Zn compound composition (%) of bulk soil, rhizospheric soil and soil obtained from LCF (d, h). ZnS, ZnS nanoparticles; ZnPhy, Zn phytate; $ZnSO_4$, Zn sulfate; ZnCys, Zn cysteine; ZnCit, Zn citrate; ZnForm, Zn formate; ZnPGA, Zn polygalacturonate. Error bars are standard error of duplicate rhizospheric soil and root samples analysed in the inoculated treatment.